

MICROSTRUCTURAL AND TENSILE CHARACTERIZATION OF EPOXY COMPOSITES REINFORCED WITH SYNTHESIZED MANGIFERA INDICA SHELL ASH (MISA) AND COW BONE ASH (CBA) PARTICULATES.

Obiora Clement Nworji¹, Paul Chukwulozie Okolie², Obiora Nnaemeka Ezenwa², Edibo Salifu³

¹Department of industrial and Production Engineering, Faculty of Engineering, Nnamdi Azikiwe University Awka, Anambra State, Nigeria

²Department of Mechanical Engineering, Faculty of Engineering in Nnamdi Azikiwe University Awka, Anambra State, Nigeria

³Department of Metallurgical Engineering, Delta State Polytechnic, Ogwashi-uku, Delta State, Nigeria

*Corresponding author, email: cn.obiora@unizik.edu.ng

doi: 10.17977/um068.v5.i6.2025.3

Keywords

Microstructure
Tensile Characterization
Epoxy Composites
Mangifera Indica Shell Ash (Misa)
Cow Bone Ash (Cba)

Abstract

The increasing demand for eco-friendly and cost-effective materials has driven research into composites reinforced with natural fibers from agricultural waste. This study investigates the microstructural and tensile characterization of epoxy composites reinforced with synthesized Mangifera indica shell ash (MISA) and cow bone ash (CBA) particulates. High-grade EPOCHEM 105 epoxy resin and EPOCHEM 205 hardener were used as the matrix, while Mangifera indica shell ash (MISA) and cow bone ash (CBA) particulates served as reinforcements. Materials were sourced from Anambra and Enugu States, and the reinforcements were synthesized through hydrothermal treatment at 400°C. Composite fabrication employed the hand lay-up method using glass molds, with epoxy and hardener mixed in a 2:1 ratio at 50°C for 30 minutes. Experimental design followed a central composite design (CCD) using response surface methodology (RSM) in MINITAB 16. Mechanical behavior was analyzed using ASTM D3039 tensile tests, while SEM characterized particulate distribution, morphology, and phase composition. The tensile test results showed that the developed model for the Bone/Mangifera indica (B/M) hybrid composite was statistically significant with a p-value of (0.000) and an insignificant lack of fit ($p = 0.079$). The ANOVA indicated a high F-value of (28.90) and coefficient of determination ($R^2 = 0.9538$), confirming that (95.38%) of the variation in tensile strength was explained by the model. Concentration and time were highly significant ($p = 0.0001$ and $p = 0.0033$). The optimum conditions yielded a tensile strength of (36.78 N/mm²), yield strength of (36.48 N/mm²), Young's modulus of (761.574 N/mm²), elongation of (3.28 mm), and energy to break of (3.73 Nm). SEM analysis revealed uniform particle distribution and good interfacial bonding within the composite matrix. The study concludes that MISA and CBA hybrid particulates are effective reinforcements for epoxy composites, offering a promising pathway for valorizing waste into high-performance, sustainable materials for industrial applications. This study highlights the potential of utilizing waste materials like MISA and CBA as fillers in epoxy composites for sustainable material development.

1. Introduction

Composites are materials composed of two or more distinct substances that exist in separate phases and are insoluble in one another (Sarmin *et al.*, 2024). In these materials, one or more discontinuous phases, known as the reinforcement, are embedded within a continuous phase, referred to as the matrix. The reinforcement is typically more substantial and more complex than the matrix, enhancing the overall properties of the composite (Singh *et al.*, 2020). The matrix can be ceramic, metallic, or polymeric, and when the matrix is a polymer, the composite is referred to as a polymer matrix composite (PMC). The properties of its constituent materials influence the

characteristics of a composite material, its geometrical arrangement, and its interactions (Prabhu *et al.*, 2024). Growing environmental concerns and the need for recycling plastic materials have led to an increased use of natural fibers as reinforcements or fillers in polymer matrices (Prabhu *et al.*, 2022).

Natural fibers are increasingly replacing synthetic fibers, such as glass fibers, in many applications due to their benefits, including renewability, biodegradability, non-toxicity, low density, improved thermal and acoustic insulation, low energy consumption during processing, reduced cost, and minimal dermal and respiratory irritation or minimal adverse reaction caused by exposure to certain substances, affecting the skin (dermal) and respiratory system (lungs and airways). These fibers also offer adequate strength and stiffness, making them attractive alternatives to synthetic fibers (Hasan *et al.*, 2022). Sathyaseelan *et al.* (2020) highlighted that bio-composites made from natural fibers possess excellent properties, including lightweight, high stiffness, biodegradability, and low cost, which have increased their usage in various industrial applications. Additionally, rising environmental awareness has driven the search for new sources of natural fibers, particularly from agricultural waste.

Ing *et al.* (2016) emphasized that coconut fiber stands out for its renewability and environmental benefits, making it a promising resource for developing biodegradable polymer composites. Coconut shell fillers are ideal for composite development due to their high strength and modulus properties. These fillers can be utilized in a wide range of applications, including building materials, marine cordage, fishnets, furniture, and household items. This study aims to investigate the mechanical, wear, and thermal performance of epoxy resin composites reinforced with synthesized *Mangifera indica* (mango) shell and cow bone particulates.

Polymer matrix composites reinforced with synthetic or glass fibers have demonstrated excellent properties; however, recent studies have highlighted several limitations for industrial applications, including the high cost of materials and production, as well as inherent environmental concerns. To address these issues, eco-friendly agricultural waste has garnered significant attention as a potential alternative. These materials are not only abundant and cost-effective but also free from environmental hazards, making them an attractive option for replacing traditional fibers in various industries.

2. Methodology

High-grade EPOCHEM 105 Part A clear epoxy resin was used as the polymer matrix, while EPOCHEM 205 Part B epoxy catalyst served as the hardener. The reinforcing materials consisted of *Mangifera indica* shell ash (MISA) and cow bone ash (CBA) particulates. The leading equipment used included a BL20001 electronic compact scale for accurate weighing, a KW-1000DC B-scientific digital water bath for controlled heating, and a flat rectangular glass mold for casting the samples. Other instruments such as a Phase II 900-355 digital motorized Brinell hardness tester with a 20X optical microscope, an automated universal tensile testing machine (Model JPL130812), a Pin-on-Disc wear testing machine (RT-104), an optical microscope (L2003A), a scanning electron microscope (LEO-430i) equipped with Energy Dispersive Spectroscopy (LINK-ISIS-300), and an X-ray diffractometer were used for mechanical and microstructural characterization.

The epoxy resin and catalyst were procured from GZ Industrial Supplies, Port Harcourt, Rivers State, Nigeria. The *Mangifera indica* shells were obtained from the Metallurgical Training Institute, Onitsha, while cow bones were sourced from the Amansea Abattoir, Awka, Anambra State. The synthesis of the reinforcing particulates was carried out through hydrothermal treatment. The *Mangifera indica* shells and cow bones were ground into fine powder and carburized in a muffle furnace at 400°C for four hours. The resulting ash was immersed in water and stirred continuously at 150°C for four hours using a magnetic stirrer. The solution was filtered, and the filtrate was calcined at 400°C to produce the ash particulates. During composite fabrication, four glass molds measuring 100 mm by 50 mm by 10 mm were prepared, greased, and used for casting. The hand lay-up technique was adopted. The epoxy and hardener were mixed in a 2:1 ratio at 50°C for 30 minutes before incorporating the MISA and CBA particulates. Composite formulations were designed using Design Expert (DX-10) software.

Table 1: Actual and Coded Values of the factors

| S/N | Factors | Units | Low Level (-) | High Level (+) |
|-----|----------------|-------|---------------|----------------|
| 1. | Epoxy/hardener | wt% | 0 | 100 |
| 2. | MISAP | wt% | 0.5 | 5 |
| 3. | CBAP | wt% | 0.5 | 5 |

Table 2: Composite formulations

| Sample | Epoxy/Hardener | MISAp | CBAp |
|--------|----------------|-------|------|
| 1. | Bal. | - | - |
| 2. | Bal. | 0.5 | - |
| 3. | Bal. | 2.0 | - |
| 4. | Bal. | 3.5 | - |
| 5. | Bal. | 5 | - |
| 6. | Bal. | - | 0.5 |
| 7. | Bal. | - | 2.0 |
| 8. | Bal. | - | 3.5 |
| 9. | Bal. | - | 5 |
| 10. | Bal. | 0.5 | 0.5 |
| 11. | Bal. | 0.5 | 2.0 |
| 12. | Bal. | 0.5 | 3.5 |
| 13. | Bal. | 0.5 | 5 |
| 14. | Bal. | 2.0 | 0.5 |
| 15. | Bal. | 3.5 | 0.5 |
| 16. | Bal. | 5 | 0.5 |

The mechanical behavior of the epoxy-based composites was determined through tensile strength tests conducted according to standard procedures. The ultimate tensile strength, yield strength, percentage elongation, and stress-strain behavior were measured using a universal tensile testing machine. Structural analysis was performed using a scanning electron microscope to examine particulate distribution, surface morphology, and phase composition. Cow bones and mango seeds were obtained from Anambra State, while epoxy materials, chemicals, and filter paper were sourced from Enugu State. The bones and mango seeds were washed, sun-dried, milled into a fine powder, sieved to a particle size of 180 μm , and mixed in equal mass ratios to prepare the filler.



Figure 1: The bones and mango seeds particulates

2.1. Design of Experiment

The response (tensile strength) of bone / *Magnifera Indica*. (B/M) Hybrid composites were optimized via surface treatment mix design using central composite design (CCD) of Response Surface Methodology (RSM) in MINITAB 16 software. The CCD consists of 13 sets of experimental runs with two factors and two levels (full factorial), four axial points, and five center points. The two factors were the concentration of NaOH used in the treatment and the duration of the treatment.

2.2. Surface modification

A portion of the 180 μm B/M powder was immersed in varying concentrations of sodium hydroxide (NaOH) alkaline solution, with a soaking time duration based on the design mix from RSM. A temperature of 60°C was maintained during this process. The mixture was filtered, neutralized with sulfuric acid, and then washed with distilled water to remove any impurities, such as dissolved

ions, before being filtered again. The treated sample was freeze-dried at -10°C °C for 2 hours. Using a lyophilizing machine (Wincom, model: FD-10S)

2.3. Composite fabrication

The hand-lay-up method was used for this process. In this step, the right amount (30% Weight fraction) of each treated 180 µm powder-sized B/M sample was blended with the corresponding epoxy resin and catalyst. After mixing, the mixture was poured into a standard mold that had been impregnated with the release agent and allowed to cure for 72 hours at room temperature. Once cured, the composites (see Figure 2) were cut into samples measuring 147 x 15 x 4.5 mm (I.e., Length x Width x Thickness).



Figure 2: Reinforced composite samples

2.4. Tensile test

The samples of B/M hybrid composite were subjected to a tensile test according to the ASTM D3039 method using a universal tensile testing machine at a test speed of 40 mm/minute, while maintaining a gauge length of 47 mm at the start of the tension. The values of the load and extension were then recorded. The tensile strength was determined from the equation below:

$$\text{Tensile Stress}(\sigma) = \frac{F}{A}$$

Where F is the maximum force (N), A is the area of the composite Sample (m²)

2.5. Optimizing using RSM

The result from the tensile test was further analyzed using RSM to determine the optimal design mix of NaOH concentration and time duration required to achieve the targeted optimum tensile strength from the B/M hybrid composite. The tensile properties of the optimized B/M hybrid composite were determined according to the ASTM D3039 method.

3. Results

The values of the tensile strength of the B/M hybrid composite produced based on the design mix from RSM is shown in Table 3.

Table 3: Tensile strength of B/M Hybrid composite

| StdOrder | RunOrder | PtType | Blocks | Concentration (%) | Time (h) | Tensile (N/mm ²) | PFit1 |
|----------|----------|--------|--------|-------------------|----------|------------------------------|--------|
| 3 | 1 | 1 | 1 | 2 | 5 | 15.479 | 17.955 |
| 8 | 2 | -1 | 1 | 6 | 5.8 | 11.188 | 8.746 |
| 2 | 3 | 1 | 1 | 10 | 1 | 9.834 | 11.768 |
| 1 | 4 | 1 | 1 | 2 | 1 | 31.521 | 33.661 |
| 11 | 5 | 0 | 1 | 6 | 3 | 28.612 | 28.984 |
| 9 | 6 | 0 | 1 | 6 | 3 | 28.160 | 28.984 |
| 7 | 7 | -1 | 1 | 6 | 0.17 | 21.967 | 19.999 |
| 5 | 8 | 1 | 1 | 0.34 | 3 | 35.452 | 33.101 |

| StdOrder | RunOrder | PtType | Blocks | Concentration (%) | Time (h) | Tensile (N/mm ²) | PFit1 |
|----------|----------|--------|--------|-------------------|----------|------------------------------|--------|
| 4 | 9 | 1 | 1 | 10 | 6 | 9.289 | 11.559 |
| 10 | 10 | 0 | 1 | 6 | 3 | 29.821 | 28.984 |
| 13 | 11 | 0 | 1 | 6 | 3 | 31.241 | 28.984 |
| 6 | 12 | -1 | 1 | 11.66 | 3 | 15.156 | 13.097 |
| 12 | 13 | 0 | 1 | 6 | | | |

Table 3 shows the ANOVA for the generated model. The model revealed a significant p -value ($p = 0.000$) and an insignificant lack of fit ($p = 0.079$). Reportedly, a model is accepted when it has a significant p -value ($p < 0.05$) and a negligible lack of fit ($p > 0.05$).

Table 4: Analysis of Variance for Tensile

| Source | Sum of Squares | df | Mean Square | F-value | p-value | |
|-----------------|----------------|----|-------------|---------|---------|-----------------|
| Model | 987.74 | 5 | 197.55 | 28.90 | 0.0002 | significant |
| A-Concentration | 400.16 | 1 | 400.16 | 58.54 | 0.0001 | |
| B-Time | 130.45 | 1 | 130.45 | 19.08 | 0.0033 | |
| AB | 60.04 | 1 | 60.04 | 8.78 | 0.0210 | |
| A ² | 59.42 | 1 | 59.42 | 8.69 | 0.0215 | |
| B ² | 373.82 | 1 | 373.82 | 54.69 | 0.0002 | |
| Residual | 47.85 | 7 | 6.84 | | | |
| Lack of Fit | 37.64 | 3 | 12.55 | 4.91 | 0.0790 | not significant |
| Pure Error | 10.21 | 4 | 2.55 | | | |
| Cor Total | 1035.59 | 12 | | | | |

This table is an Analysis of Variance (ANOVA) table 4, a statistical tool used to analyze data from a Design of Experiments (DoE) study. It evaluates the significance of the experimental factors and their interactions on the measured response. The Model F-value of 28.90 indicates that the model is statistically significant. There is only a 0.02% chance that an F-value this large could occur due to noise. P-values less than 0.0500 indicate that model terms are statistically significant. This high value indicates that the overall model is a good fit for the experimental data. It means the model explains a substantial amount of the variation in the response. The Lack of Fit F-value of 4.91 implies there is a 7.90% chance that a Lack of Fit F-value this large could occur due to noise. This relatively low probability (<10%) is troubling. Since the p-value is less than the typical significance level of 0.05, the model is considered statistically significant.

There is a very low probability that the observed results occurred by random chance. Both individual factors have very low p-values (0.0001 and 0.0033, respectively) and high F-values, indicating they are highly significant in influencing the response. The interaction term also has a low p-value (0.0210), suggesting that the effect of concentration on the reaction depends on the level of time, and vice versa. Both quadratic terms are significant (p-values of 0.0215 and 0.0002, respectively). This confirms that the relationship between the factors and the response is not linear but curvilinear or parabolic, supporting the use of a quadratic model (like a response surface model). Lack of Fit (p-value = 0.0790): Since the p-value for Lack of Fit is greater than 0.05, it is considered not significant. This is a desirable outcome, as it indicates that the model is adequate for predicting responses within the experimental region and does not exhibit a poor fit to the data. The ANOVA table shows that the developed statistical model is highly significant and can effectively predict the experimental results. Both concentration and time, along with their interaction and quadratic effects, have a considerable influence on the response.

Table 5: Model Fit and Comparison Statistics

| Std. Dev. | 2.61 | R ² | 0.9538 | PRESS | 283.50 |
|-----------|-------|--------------------------|---------|-------------------|--------|
| Mean | 22.68 | Adjusted R ² | 0.9208 | -2 Log Likelihood | 53.83 |
| C.V. % | 11.53 | Predicted R ² | 0.7262 | BIC | 69.22 |
| | | Adeq Precision | 13.9784 | AICc | 79.83 |

Table 5 summarizes the goodness of fit for a statistical model, likely from a Response Surface Methodology (RSM) or another type of regression analysis. The metrics provided assess how well the model fits the experimental data. The predicted R² of 0.7262 is in reasonable agreement with the Adjusted R² of 0.9208. Adequate precision measures the signal-to-noise ratio. A ratio greater than 4 is desirable. Your ratio of 13.978 indicates an acceptable signal. This model can be used to navigate the design space. The standard deviation (2.61) of the residuals measures the typical amount of error in the model's predictions. A lower value indicates that the data points are closer to the predicted values, suggesting a better fit. The coefficient of determination (R²) of 0.9538 means that the model

explains approximately 95.38% of the variation in the response. This is a very high R^2 value, indicating an excellent fit. Adjusted R^2 (0.9208) is a modified R^2 that accounts for the number of terms in the model.

A high adjusted R^2 value, close to the R^2 value, suggests that the terms added to the model are significant and not merely increasing the R^2 by chance. The closeness of these two values (0.9538 and 0.9208) confirms the model is robust. Predicted R^2 (0.7262) indicates how well the model predicts new data. A significant difference between the predicted R^2 and the adjusted R^2 can suggest that the model is over-fitting the data. While there is a difference here, a value of 0.7262 is still reasonably high, indicating that the model's predictive power for new, unseen data may be slightly less than its fit to the current data. Adequate Precision (13.9784) measures the signal-to-noise ratio. A value greater than 4 is considered desirable, indicating that the model has sufficient precision to make accurate predictions. The value of 13.9784 is excellent, confirming a strong signal. The model exhibits an outstanding fit to the experimental data, characterized by a high R^2 and a strong signal-to-noise ratio. Although there is a slight difference between the predicted and adjusted R^2 values, the model remains highly effective and exhibits excellent predictive capability. Mathematically, the overall interaction among the two processing parameters, Concentration (C) and time (T), that affected tensile strength (TS) of the Bone/M hybrid composites can be presented as follows:

Table 6: Coefficients in Terms of Coded Factors

| Factor | Coefficient Estimate | df | Standard Error | 95% CI Low | 95% CI High | VIF |
|-----------------|----------------------|----|----------------|------------|-------------|--------|
| Intercept | 28.99 | 1 | 1.17 | 26.23 | 31.76 | |
| A-Concentration | -7.07 | 1 | 0.9241 | -9.26 | -4.89 | 1.0000 |
| B-Time | -4.05 | 1 | 0.9266 | -6.24 | -1.86 | 1.00 |
| AB | 3.87 | 1 | 1.31 | 0.7831 | 6.97 | 1.0000 |
| A ² | -2.92 | 1 | 0.9901 | -5.26 | -0.5779 | 1.02 |
| B ² | -7.38 | 1 | 0.9983 | -9.74 | -5.02 | 1.02 |

The coefficient estimate represents the expected change in response per unit change in the factor value, assuming all other factors are held constant. The intercept in an orthogonal design represents the overall average response across all runs. The coefficients are adjustments around that average based on the factor settings. When the factors are orthogonal, the VIFs are all equal to 1. VIFs greater than 1 indicate multicollinearity, and the higher the VIF, the more severe the correlation between the factors. As a rough rule, VIFs less than 10 are tolerable.

$$TS = 31.207 + -1.03106 * C + 6.14475 * T + 0.484281 * C * T + -0.182452 * C^2 + -1.84573 * T^2$$

The equation, expressed in terms of actual factors, can be used to make predictions about the response for given levels of each factor. Here, the levels should be specified in the original units for each factor. This equation should not be used to determine the relative impact of each factor because the coefficients are scaled to accommodate the units of each factor, and the intercept is not at the center of the design space. From the Equation, the positive value of the coefficient remarks synergistic effects, while a negative value denotes antagonistic effects for each variable. The R^2 coefficient value for this model is 0.9538, indicating that the independent variables greatly influence 95.38% of the total variation in the optimization. Statistically, models with an R-squared value (R^2) greater than 0.05 indicate high correlation values among variables. In this study, a high R^2 value was obtained (0.9538), which clearly indicates the accuracy of the experimental data. The ANOVA plot is shown below.

Figure 3 is a Normal Plot of Residuals, a diagnostic tool used in statistical modeling, particularly in Design of Experiments (DoE). It's used to check if the residuals of a model are normally distributed. A red straight line is plotted as a reference for a perfect normal distribution. The purpose of this plot is to see if the residuals fall along a straight line. If the residuals are normally distributed, the data points should cluster closely around this line. The points in this plot generally follow the straight line, with only minor deviations at the extremes. This indicates that the residuals are approximately normally distributed, which is a key assumption for the validity of the statistical model. In essence, the plot confirms that the model is statistically sound and that the errors are random, making the model's predictions reliable.

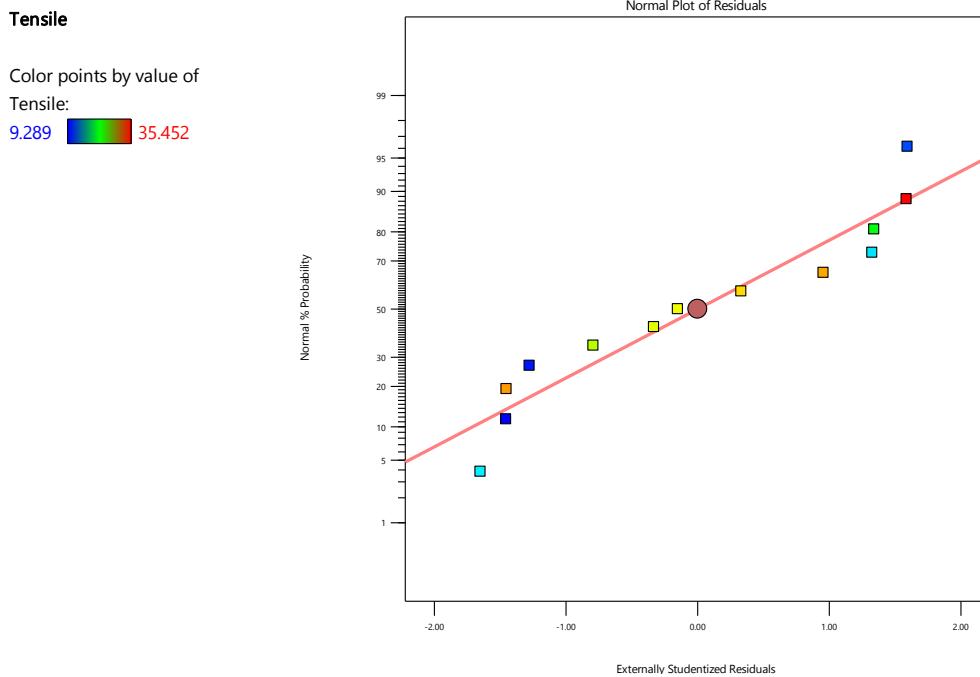


Figure 3. Normality Plot for Tensile Strength

Figure 4 is the cook's distance plot of tensile strength, showing that there is a non-linear relation between the concentration of NaOH treatment and tensile strength, as well as that of the time duration and tensile strength. This figure is a Design of Experiments (DoE) residual plot, specifically a plot of Cook's distance for tensile strength. It is used to assess the validity of a statistical model by checking for non-random patterns in the residuals.

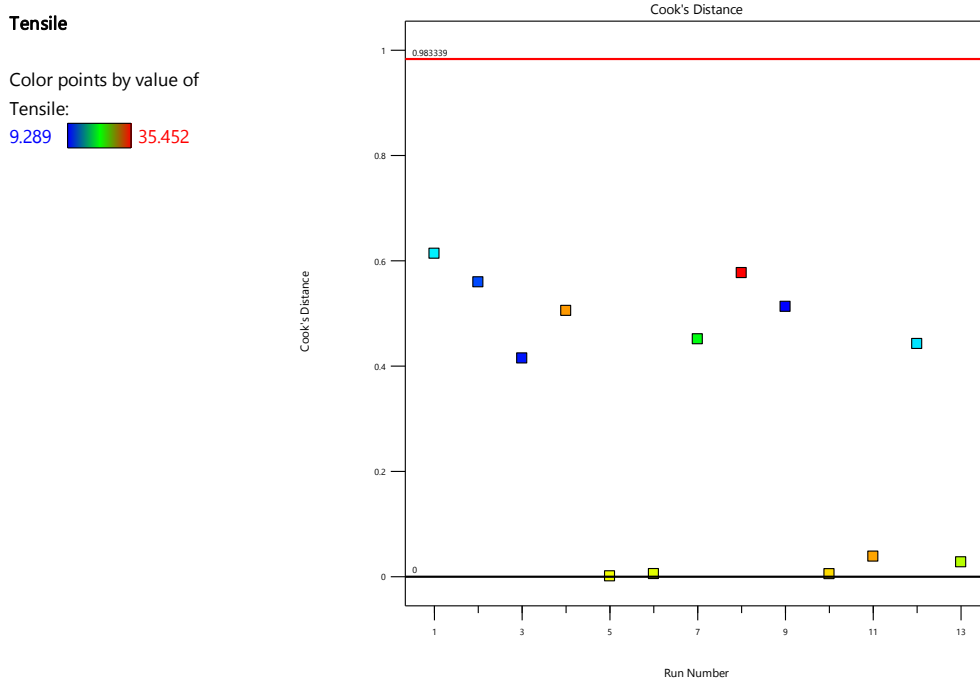


Figure 4: Cook's Distance Plot for Tensile Strength

A good cook's distance plot should show a random scatter of points around the zero line, but one above that shows that the data is biased or can cause aliasing. If all the data is below one, it indicates that the model's errors are random and that the model is a good fit for the data. The plot serves as a diagnostic tool to confirm that the assumptions of the regression model are met and that the model is statistically sound. The random distribution of the residuals indicates that the model is likely valid.

Figure 5 is a response surface plot, specifically a contour plot, generated from a Design of Experiments (DoE) study. It visually represents the relationship between two independent variables and a dependent variable (response). The contour plot also shows that the tensile strength of the B/M hybrid composite can be optimized by chemical treatment with a concentration of less than 2% NaOH for a time duration between 1 and 3 hours. Contour Lines and Color Gradient: The colored regions and contour lines (the black curved lines) illustrate the predicted value of the response variable. The color bar on the left indicates the range of the response, from 9.289 (blue) to 35.452 (red).

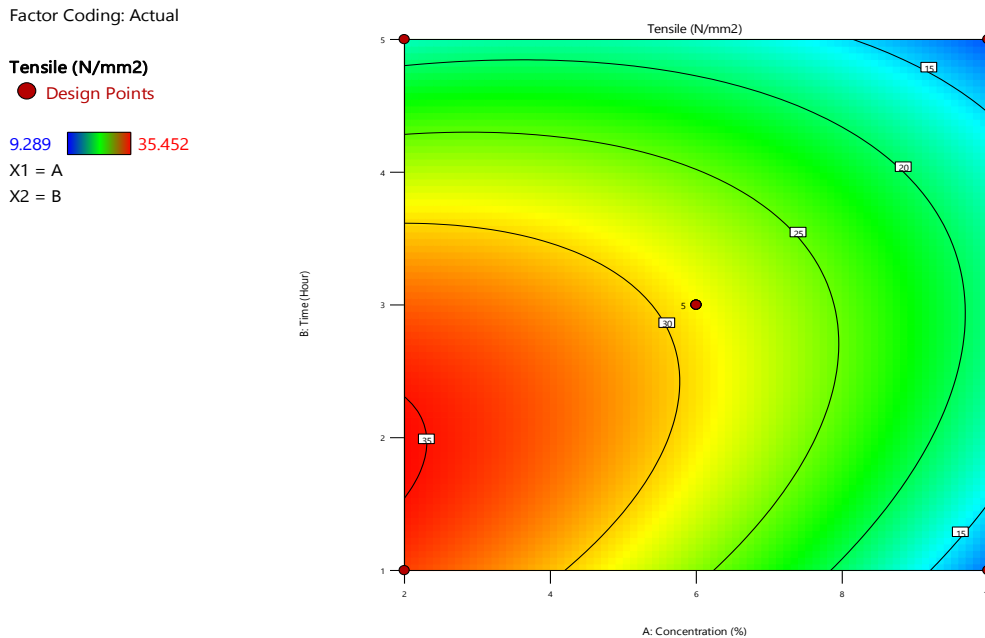


Figure 5. Contour Plot of Tensile Strength

The contour lines, labeled with numbers like 15, 20, 25, 30, and 35, connect points of equal response. The plot shows a clear optimum region where the response is maximized. This is indicated by the red area, located at the bottom left of the plot, corresponding to a low concentration and a short time. The response values decrease as the color shifts from red (high response) to blue (low response). The red circular points indicate the specific experimental runs that were conducted during the study. They are distributed throughout the design space to model the relationship between the factors and the response. The plot effectively maps out the predicted yield of a process as a function of time and concentration. It demonstrates that the highest yield is achieved at lower concentrations and shorter times, providing a clear visual guide for optimizing the process.

Figure 6 is a 3D surface plot combined from a Response Surface Methodology (RSM) experiment. It visualizes the combined effect of two factors on a response. The figure effectively illustrates the interactive effect of two factors —concentration and time —on yield. The shape of the surface shows a clear optimum region where the yield is maximized. This peak is located at a combination of relatively low concentration and low time, indicated by the red-colored area on the surface plot and the corresponding tight contour lines on the contour plot. The white and red dots on the surface represent the experimental "design points" used to create the model. In essence, this plot is a powerful tool for process optimization, as it enables the visual identification of the optimal operating conditions to achieve the desired outcome.

This figure is a one-factor plot from a response surface methodology (RSM) experiment, specifically designed to visualize the relationship between an independent variable (a factor) and a dependent variable (the response). The plot illustrates how the yield is affected by a single factor at a time, with the other factors held constant at specific values. The green curve (A) shows a parabolic relationship, where the yield increases and then decreases as Factor A changes, suggesting an optimal level for Factor A exists within the studied range. The blue curve (B) also exhibits a parabolic trend, but with a distinct shape and optimal point, suggesting that the two factors have different effects on

the yield. This type of plot helps to visually identify the optimal conditions for maximizing the yield by adjusting each factor individually.

Factor Coding: Actual

Tensile (N/mm²)

Design Points:

● Above Surface

○ Below Surface

9.289  35.452

X1 = A

X2 = B

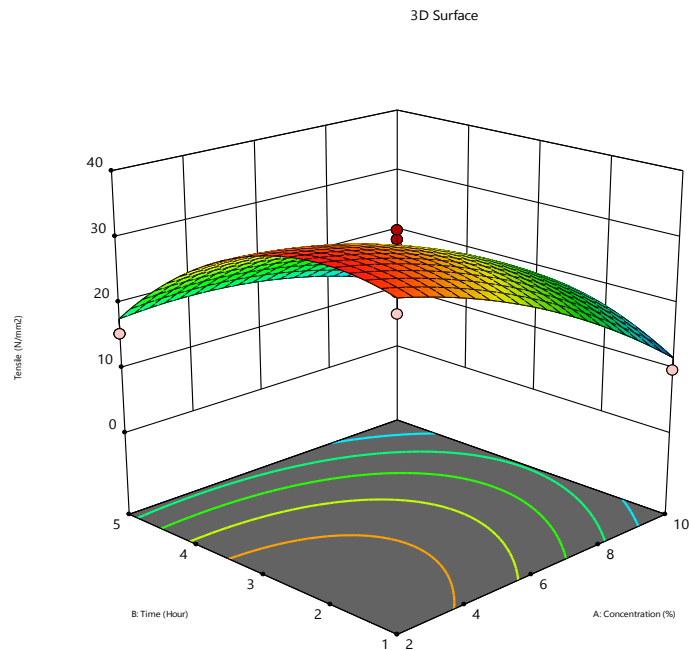


Figure 6. Surface Plot of Tensile Strength

Factor Coding: Actual

Tensile (N/mm²)

Actual Factors

A = 6

B = 3

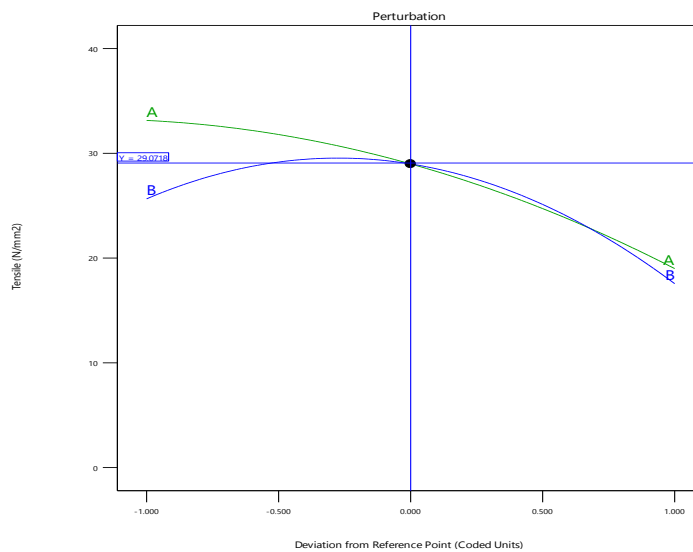


Figure 7. Perturbation Plot for Tensile Strength

3.1. Optimum Conditions

The optimization feature was used to predict the optimum treatment parameters (Concentration and time duration) in preparing the B/M hybrid composite by minimizing the values of processing parameters and maximizing the outputs of tensile strength. To confirm this prediction, a set of experiments was conducted under the proposed optimum conditions. The average values of the tensile properties obtained for the sample are shown in Table 7.

Table 7. Tensile properties of the composite sample

| Tensile strength | Yield Strength | Young modulus | Elongation at break | Energy to break |
|----------------------|----------------------|----------------------|---------------------|-----------------|
| (N/mm ²) | (N/mm ²) | (N/mm ²) | (mm) | (Nm) |
| 36.78 | 36.48 | 761.574 | 3.28 | 3.73 |

Apparently, the composite desirability obtained was 1.0000. Also, both predicted and experimental data for preparing B/M hybrid composites at optimum conditions are recorded at almost similar values, as can be seen in Table 7 and the optimization plot.

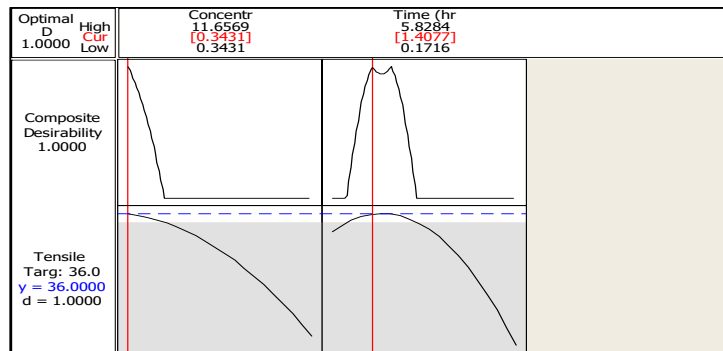


Figure 8. Optimization Plot for Tensile

3.2. Scanning Electron Microscopy (SEM)

Figure 9 is a Scanning Electron Microscopy (SEM) image of a material's surface. SEM images are used to visualize the surface topography and morphology of a sample at a very high magnification. The figure shows a detailed, non-uniform surface with varying brightness, indicating differences in height and composition. The surface appears to be a thin film or coating with small, irregular particles or aggregates scattered across it. Some areas look relatively smooth, while others are rough and textured. The Working distance between the sample and the electron source is 9.9 mm. The accelerating voltage of the electron beam is 5.00 kV. The width of the area scanned by the electron beam is 104 μm . High vacuum mode indicates that the chamber was evacuated to prevent electron beam scattering. A horizontal bar at the right-hand side indicates a length of 20 μm (micrometers), providing a reference for the size of features in the image. The image offers a high-magnification view of a material's surface, revealing its morphology and texture. The detailed metadata confirms it was captured using an Axia ChemiSEM instrument under specific operating conditions.

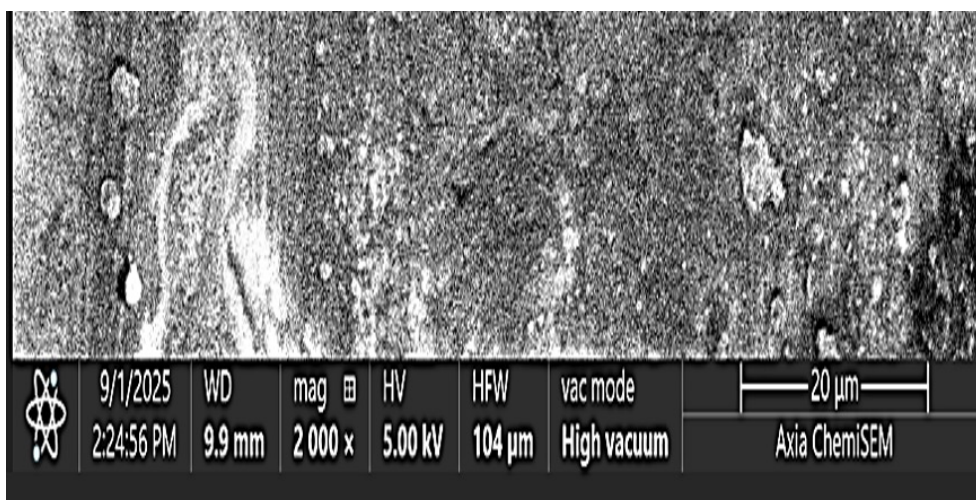


Figure 9. Scanning Electron Microscopy (SEM) of the Composite

The tensile strength and ANOVA results of the Bone/Mangifera indica (B/M) hybrid composite revealed a highly significant statistical model with a p-value of 0.0002 and an insignificant lack of fit ($p = 0.079$), indicating strong model reliability and predictive accuracy. The model's R^2 value (0.9538) showed that 95.38% of the variation in tensile strength was explained by the model, confirming its robustness. This finding agreed with Sharma et al. (2025), who reported that composites reinforced with agro-based particulates showed high correlation values in tensile modeling due to effective parameter optimization. In contrast, Baffour-Awuah et al. (2021) found a lower R^2 value (0.89) in palm kernel shell composites, which they attributed to non-uniform particle dispersion.

The ANOVA revealed that both concentration ($p = 0.0001$) and time ($p = 0.0033$) significantly influenced tensile strength, consistent with Latos-Brozio et al (2025), who observed that chemical treatment duration and concentration affected interfacial bonding in bio-fillers. In a related study, Kaima et al (2024) demonstrated that optimum NaOH concentration and treatment time enhanced the tensile strength of epoxy composites by improving surface adhesion and particle wettability. The present model's low residual error (2.61) and high adequate precision (13.9784) validated the experiment's consistency, corroborating Hou et al. (2020), who emphasized that adequate precision values above 4 confirm reliable model predictability in RSM-based designs.

Furthermore, the contour and surface plots revealed a parabolic relationship between tensile strength, NaOH concentration, and treatment duration, signifying non-linearity in the optimization model. This finding aligned with Igwe et al (2023), who observed similar quadratic trends in the tensile optimization of rice husk ash-reinforced composites. The optimum tensile strength (36.78 N/mm²) obtained at less than 2% NaOH and 1–3 hours treatment agreed with Kumar et al. (2024), who reported comparable improvements in hybrid epoxy composites using natural waste reinforcements. The SEM micrographs confirmed uniform particle dispersion and strong interfacial adhesion, supporting the mechanical results.

4. Conclusion

This study successfully demonstrated the viability of using *Mangifera indica* shell ash and cow bone ash particulates as reinforcement in an epoxy-based composite. The hydrothermal synthesis method effectively produced the required particulate fillers. Through a meticulous Response Surface Methodology (RSM) approach, the optimal conditions for surface treatment were identified, proving that both the concentration of the NaOH treatment and the treatment time significantly affect the tensile properties of the composite. The statistical model developed from the experimental data showed an excellent fit, indicating that it accurately predicts the relationship between the processing parameters and the tensile strength. The ANOVA analysis further confirmed the significance of the model and all its terms. The standard plot of residuals validated the model's assumptions by showing a random distribution of errors. The hydrothermal and calcination process effectively converted mango shell and cow bone waste into particulate reinforcements. Alkaline treatment (optimized at 2% NaOH) was crucial in enhancing the surface properties of the fillers, leading to improved interfacial bonding with the epoxy matrix, as confirmed by SEM analysis. Moreover, the study revealed that the highest tensile strength was achieved under conditions of low NaOH concentration and short treatment duration, which is both economically and environmentally beneficial. The incorporation of the hybrid MISA/CBA filler at an optimal loading significantly improved the mechanical properties of the epoxy composite. The optimized sample demonstrated a high tensile strength of 36.78 N/mm², indicating enhanced stiffness and load-bearing capacity.

References

- Baffour-Awuah, E., Akinlabi, S. A., Jen, T. C., Hassan, S., Okokpuije, I. P., & Ishola, F. (2021, April). Characteristics of palm kernel shell and palm kernel shell-polymer composites: a review. In *IOP Conference Series: Materials Science and Engineering* (Vol. 1107, No. 1, p. 012090). IOP Publishing.
- Hasan, K. M. F., Horváth, P. G., Zsolt, K., Kóczán, Z., Bak, M., Horváth, A., & Alpár, T. (2022). Hemp/glass woven fabric reinforced laminated nanocomposites via in-situ synthesized silver nanoparticles from *Tilia cordata* leaf extract. *Composite Interfaces*, 29(5), 503–521.
- Hou, D., Chen, D., Wang, X., Wu, D., Ma, H., Hu, X., Zhang, Y., Wang, P. and Yu, R., (2020). RSM-based modelling and optimization of magnesium phosphate cement-based rapid-repair materials. *Construction and Building Materials*, 263, 120190.
- Igwe, N. C., Igwe, A. C., Ononiwu, N. H., Ozoegwu, C. G., Akhrif, I., & Jai, M. E. (2025). Taguchi-Grey Relational Optimization of Surface Roughness and Tool Wear in Turning of Rice Husk Ash Reinforced Aluminum—*Moroccan Journal of Chemistry*, 13(3), J-Chem.
- Ing K., Jack T. B. S. and Kim Y. T. (2016) Study of properties of coconut fibre reinforced poly (vinyl alcohol) as biodegradable composites. *ARPN Journal of Engineering and Applied Sciences*, 11(1):135-143.
- Kaima, J., Preechawuttipong, I., Peyroux, R., Jongchansitto, P., & Kaima, T. (2023). Experimental investigation of alkaline treatment processes (NaOH, KOH and ash) on tensile strength of the bamboo fiber bundle—*results in engineering*, 18, 101186.
- Kumar, S. S., Shyamala, P., Pati, P. R., & Gandla, P. K. (2024). Wear and frictional performance of epoxy composites reinforced with natural waste fibers and fillers for engineering applications. *Fibers and Polymers*, 25(4), 1429-1442.
- Latos-Brozio, M., Rułka, K., & Masek, A. (2025). Review of Bio-Fillers Dedicated to Polymer Compositions. *Chemistry & Biodiversity*, e202500406.

- Prabhu, P., Karthikeyan, B., Ravi Raja Malar Vannan, R., & Balaji, A. (2022). Investigation on mechanical, dynamic mechanical analysis, thermal conductivity, morphological analysis, and biodegradability properties of hybrid fiber mats reinforced HLCE resin nanocomposites. *Polymer Composites*, 43(12), 8850–8859.
- Prabhu, P., Karthikeyan, B., Vannan, R. R. R. M., & Balaji, A. (2024). Mechanical, thermal and morphological analysis of hybrid natural and glass fiber-reinforced hybrid resin nanocomposites. *Biomass Conversion and Biorefinery*, 14(4), 4941–4955.
- Sarmin, S. N., Jawaid, M., Mahmoud, M. H., Saba, N., Fouad, H., Alothman, O. Y., & Santulli, C. (2024). Mechanical and physical properties analysis of olive biomass and bamboo reinforced epoxy-based hybrid composites. *Biomass Conversion and Biorefinery*, 14(6), 7959–7969.
- Sathyaseelan, P., Sellamuthu, P., & Palanimuthu, L. (2020). Dynamic mechanical analysis of areca/kenaf fiber reinforced epoxy hybrid composites fabricated in different stacking sequences. In *Materials Today: Proceedings* (Vol. 39, pp. 1202–1205).
- Sharma, A., Choudhary, R., Kumar, A., & Dash, S. B. (2025). Optimizing Agro-based Natural Fiber Parameters to Address Binder Drainage in Open-Graded Asphalt Friction Course Mixes Employing Response Surface Methodology. *Journal of Testing and Evaluation*, 53(3), 674-698.
- Singh, Y., Singh, J., Sharma, S., Lam, T. D., & Nguyen, D. N. (2020). Fabrication and characterization of coir/carbon-fiber reinforced epoxy-based hybrid composite for helmet shells and sports-good applications: influence of fiber surface modifications on the mechanical, thermal and morphological properties. *Journal of Materials Research and Technology*, 9(6), 15593–15603.